TRENDS IN SCIENCES 2026; 23(10): 13063
https://doi.org/10.48048/tis.2026.13063
RESEARCH ARTICLE

Process Optimization and Kinetics Study of Metals Leaching from Spent Hydrocracking Catalysts by Cell-free Medium Filtrate of *Aspergillus aculeatus*

Thanakorn Sawangchart[1], Bunyarit Meksiriporn[2] and Thanawat Sutjaritvorakul[1,3,*]

[1]*Department of Petrochemicals and Environmental Management, Faculty of Engineering, Pathumwan Institute of Technology, Bangkok 10330, Thailand*
[2]*Department of Biology, School of Science, King Mongkut's Institute of Technology Ladkrabang, Bangkok 10529, Thailand*
[3]*Department of Environmental Technology and Applied Science, Faculty of Science and Technology, Pathumwan Institute of Technology, Bangkok 10330, Thailand*

([*]Corresponding author's e-mail: thanawat@pit.ac.th)

Received: 16 December 2025, Revised: 11 February 2026, Accepted: 18 February 2026, Published: 10 May 2026

Abstract

Hydrocracking catalysts (HCC) are widely used in petrochemical refinery catalytic processes. Although these catalysts are frequently reusable, the efficacy of HCC gradually declines. This procedure leads to the production of a large amount of spent hydrocracking catalyst (SHCC), which contains valuable metals as well as hazardous chemical wastes. The pyro-hydro-metallurgical approach for metal restoration from catalyst waste is insufficient for environmental sustainability. The application of biological techniques is a more environmentally friendly strategy. Fungal leaching has emerged as an alternative method for the recovery of metals. Although metal recoveries were moderate, the use of cell-free fungal filtrate enabled rapid leaching under mild conditions, highlighting its potential as a greener and operationally simpler alternative to conventional whole-cell bioleaching. *Aspergillus aculeatus* was isolated from contaminated soil of a gold mine located in Thailand. The filtrate of the fungal culture medium was utilized for metal leaching, and this experiment was carried out using a Box-Behnken experimental design. The optimum processes included a spent catalyst density of 10% (w/v), a temperature of 50 °C, and a shaking rate of 148 rpm for 180 min, with the catalyst powder size being less than 150 µm. The predicted highest metal recovery rates of 7.98% for Al, 5.27% for Ni, 24.55% for Mo, 11.92% for Fe, and 0.93% for Zn aligned precisely with the actual experimental results. The comprehension of kinetics through the application of the shrink core model indicates that the mechanism of reactions is predominantly influenced by the surface chemical control reaction rather than the diffusion process. The leaching rates of Mo, Fe, Al, Ni, and Zn followed a descending order from highest to lowest.

Keywords: Fungal leaching, Heavy metal, Box-behnken experimental design, Spent hydrocracking catalyst, Shrink core model

Introduction

The world's petroleum fuel consumption has grown considerably, as has Thailand's. Since 1970, the capacity of crude oil refineries worldwide has been rising steadily. Following the COVID-19 pandemic in 2023, the global oil refinery capacity stood at approximately 101 million barrels per day International Energy Agency, [1]. Meanwhile, the daily capacity of crude oil refineries in Thailand was around 1.2 million barrels [1]. Petroleum oil refining processes have hiked the demand for and consumption to produce the finished goods. Among various catalysts, hydro-processing catalysts contribute significantly to the processes of petroleum products. The hydro-processing operation cluster typically comprises reaction units, gas separation units, sulfur removal units, and product fractionation

units. Approximately 80% of petroleum streams are thought to go through hydro-processing operation units. The hydrotreating operations are used strictly, they mostly refer to eliminating undesirable contaminants (sulfur, oxygen, nitrogen, and metals). In addition, the hydrocracking operations refer more precisely to decomposing complex hydrocarbon molecules into simpler ones. Fuels are refined to enable a lower sulfur concentration. The process of hydrocracking has two stages: Catalytic cracking and hydrogenation. Refineries use hydrocracking catalysts (HCC) to transform heavy oil fractions into middle distillates of superior quality and light products such as naphtha, diesel, and liquefied petroleum gas [2].

The spent catalysts have been a significant source of waste from petroleum refineries. These spent catalysts are considered hazardous materials due to the significant concentrations of different toxic metals they contain [3]. Several strategies can be employed to address the environmental issues associated with spent catalysts. These include reducing waste generation through regeneration and reuse, recovering metals, utilizing spent catalysts to create valuable materials, and implementing treatment methods for safe disposal [4]. Generally, molybdenum or tungsten, in conjunction with a nickel promoter, are the principal materials employed in the making of HCC, supported on a porous Al_2O_3/SiO_2 structure. The HCC becomes deactivated and needs to be renewed or replaced if it is unable to provide the desired quality of product. Metal poisoning, active phase sintering, metal alloying, and carbon (coke) fouling are the four major mechanisms of catalyst deactivation. The analysis conducted using the surface area and porosity analyzer (BET) indicated that the specific surface area of the used catalyst was lower than that of the fresh catalyst [4,5]. This difference could be attributed to fouling by contaminating metals. The factors mentioned above play a crucial role in substantially enhancing the occurrence of spent hydrocracking catalysts (SHCC), necessitating their treatment before disposal to ensure adherence to environmental regulations or laws such as the notification of the Ministry of Industry (The management of waste or spent materials B.E. 2566) of Thailand. The fundamental constituents of spent catalysts were analyzed through inductively coupled plasma (ICP) following a digestion method. The existing proportion of metals presents opportunities for recovery from SHCC. Nowadays, the two main metallurgical methods used to extract metals from waste petroleum catalysts are hydrometallurgy and pyrometallurgy. Strong bases or strong acids are used in the hydrometallurgical process, either alone or together with oxidants such as H_2O_2 and $KMnO_4$ [6]. The pretreatment procedures, including heating and crushing, are essential for eliminating surplus compounds from the spent catalyst. The selection of the processing method is contingent upon the desired purity and the ultimate value of the product. However, recovery methods focus not only on the attainment of optimal recovery but also on the environmental challenges. Bioleaching represents an environmentally sustainable solution for the extraction of metals from used catalysts. Utilizing microorganisms like fungi and bacteria to change solid substances is the basis for bioleaching. The process of this transformation yields recoverable, soluble components by generating either inorganic or organic acids [7,8]. The current research trend emphasizes the potential of organic acids produced by microbes as a viable alternative to traditional methods in the recycling sector, including the mining industry [9]. In earlier times, most experiments used whole fungal cells, listed in **Table 1**, and these leaching processes required many days. *Aspergillus* spp. is acknowledged as one of the most extensively utilized fungi in various processes of leaching [5,10-18]. This filamentous fungus has been utilized in the production of citric acid, gluconic acid, and oxalic acid [8]. The metals from the catalyst waste were extracted using the acids mentioned above. Based on everything mentioned above, bioleaching is thought to be more economical and environmentally benign than other traditional leaching techniques. Despite the environmental benefits associated with bioleaching compared to the pyro-hydro-metallurgical leaching methodologies, prior investigations into bioleaching have exhibited deficiencies within the leaching process itself, which is notably in duration. This provided an opportunity in this study because it chose to employ fungal medium filtrate rather than complete fungal cells in the extraction process. The goal of this research is to optimize and investigate the kinetics to enhance the bioleaching process of valuable metals from SHCC by applying the

fungal culture medium filtrate of *Aspergillus aculeatus*, which was isolated from contaminated soil.

Table 1 Fungal leaching studies carried out on spent refinery catalysts for metal recovery.

Fungal strain	Processing and/or study approach	Maximum metals leaching capacity	References
Aspergillus niger	One-step bioleaching and Two-step bioleaching	Pt 37%	H Malekian *et al*., [10]
Aspergillus niger, Aspergillus foetidus, and Aspergillus carbonarius	Batch culture processing	Al 88.43%	S Das *et al*., [5]
Aspergillus niger	One-step bioleaching	Al 50%, Ti 32%, and V 42%	MH Muddanna and SS Baral, [11]
Aspergillus niger	Spent medium bioleaching	Ni 4.7% and V 18%	MH Muddanna and SS Baral, [12]
Aspergillus niger	Kinetics and process optimization	Mo 99.5%, Ni 45.8%, and Al 13.9%	F Amiri *et al*., [13]
Penicillium simplicissimum	Process optimization	Mo 97.6%, Ni 45.7%, and Al 14.3%	F Amiri *et al*., [14]
Penicillium simplicissimum	Two-step bioleaching	W 100%, Fe 100%, Mo 92.7%, Ni 66.43%, and Al 25%	F Amiri *et al*., [15]
Aspergillus niger	One-step bioleaching	Ni 78.5%, Mo 82.3%, and Al 65.2%	D Santhiya and YP Ting, [16]
Aspergillus niger	One-step bioleaching and Two-step bioleaching	Al 54.5%, Ni 58.2%, and Mo 82.3%	D Santhiya and YP Ting, [17]
Aspergillus niger	Batch culture processing	Ni 9%, Fe 23%, Al 30%, V 36%, and Sb 64%	KMM Aung and YP Ting, [18]

Materials and methods

Spent hydrocracking catalyst powder

The received SHCC was supplied by NICS Innovation Company. It was collected from refineries in the Eastern Economic Corridor (EEC) of Thailand. Initially, the metal composition of the raw SHCC will be evaluated utilizing a Vanta® handheld XRF analyzer. However, this SHCC is inappropriate for the leaching stage because of the presence of coke and oil covering its surface. Pre-treatment: The black-covered spent catalyst was heated at 600 °C for 6 h in a furnace [19]. It was carefully powdered and sieved with a stainless-steel wire mesh. Spent catalyst with particle size less than 150 µm was used in this experiment [15]. A sample weighing between 0.02 and 0.05 g was subjected to digestion for 2 h in a mixture of 10 milliliters of concentrated nitric acid and 10 milliliters of concentrated hydrofluoric acid. Following this, the sample was subjected to a temperature of 120 °C for an additional 2 h. The majority of the sample dissolved in the digestion solution [15]. After cooling, the digestate was subjected to filtration and subsequently brought to a final volume of 100 milliliters with water that had been purified or deionized. Subsequently, the sample underwent chemical analysis via an ICP-AES (ICPE-9820® Shimadzu).

Isolation, screening, and identification of fungi

Fungi were isolated from polluted soil gathered from a gold mine in Phichit province, Thailand. The soil

sample was kept in a sterile plastic bag and stored at 4 °C for fungal isolation. A total of 50 g of soil was combined with 100 mL of sterile 85% NaCl solution and mixed thoroughly by shaking. The fungi were isolated from the soil solution by the serial dilution plating method as described in the report by Aziz [20]. After evenly spreading the solution across the potato dextrose agar (PDA) plate, the solution was incubated for 7 days at room temperature (25 °C). After incubation time, fungal colonies from the original culture were moved to new medium plates in order to obtain a pure culture of fungi. PDA medium supplemented with 0.5% (w/v) SHCC was used to cultivate all isolate fungal strains for seven days at room temperature. The pure cultures of any fungal isolates that were able to grow were collected for further research [21,22]. In the morphology-based identification techniques, the fungi were examined through the analysis of fungal characteristics using light microscopy [23]. For molecular genetics identification, the isolate was identified by confirmation through molecular techniques. A modified cetyl trimethyl ammonium bromide (CTAB) extraction method was used to separate total genomic DNA from fungal strains [24]. A polymerase chain reaction (PCR) was performed on the extracted DNA samples to amplify the internal transcribed spacer (ITS) regions. The following universal primers will be used: ITS1 (Forward Primer): TCC GTA GGT GAA CCT GCG G, and ITS4 (Reverse Primer): TCC TCC GCT TAT TGA TGA TAT GC. PCR was carried out at 94 °C for three min, followed by 30 cycles of denaturation at 94 °C for 30 s, annealing at 56 °C for one min, and extension at 72 °C for one min. In the final step, each isolate's ITS and 18S rRNA genes were amplified and sequenced at 72 °C for 10 min [8]. Subsequently, these sequences were compared against the GenBank databases and aligned with the reference sequences.

Fungal culture medium filtrate preparation

In a conical flask containing potato dextrose broth (PDB) at pH 6.5, isolated fungi were cultured and incubated on a rotary shaker at a speed of 150 rpm and a temperature range of 30 to 35 °C for 9 days. After the incubation period, the mycelium was filtered, and the culture medium filtrate was centrifuged for 10 min at a speed of 10,000 rpm. During the incubation period, samples of the culture medium were monitored to assess the levels of organic acids and to measure changes in pH. The citric and oxalic acid measurements were performed using a Prominence HPLC system (Shimadzu, Japan), operated via a workstation utilizing Lab Solutions software. This system had a UV/VIS diode array detector adjusted to a wavelength of 210 nm [25].

Leaching process optimization and kinetics

The leaching process took place in 250 mL Erlenmeyer flasks filled with SHCC powder in 100 mL autoclaved culture filtrate. Before sterilization, the filtrate was modified to a pH of 6.5 by adding 2 N HCl. The experiments were performed using an orbital shaking incubator, in which several parameters, including catalyst pulp density, shaking rate, and temperature, were methodically altered for 180 min, following the Box-Behnken design [26]. The proportion of catalyst to volume was modified at pulp densities of 3%, 6%, and 10% (w/v). Shaking rates of the incubator were varied at 120, 150, and 180 rpm. The temperature of experiments in an incubator was changed from 30, 40, to 50 °C. Three replicates were employed to examine these various leaching studies. A control experiment was carried out with a pulp density of 10% w/v (SHCC powder in free-cell culture medium), a shaking rate of 180 rpm, and a temperature of 50 °C.

Upon completion of the incubation period, a filtration process was used to obtain culture filtrates. These filtrates have been determined using an ICP-AES (ICPE-9820® Shimadzu) for metal ions. The proportion of metal recovery was calculated using the formula provided in Eq. (1) [5].

$$\% R_{metal} = (C_M / C_{SHCC}) \times V_M \times 100 \quad (1)$$

where % R_{metal} is the percentage of metal recovery from the SHCC. C_M (mg/L) is the concentration of the leached metal in the medium filtrate; V_M is the volume of the medium, which is 100 mL (0.1 L); C_{SHCC} (mg) is the metal content in the SHCC, which has been determined by ICP-AES of pretreated SHCC, in this study.

The experimental design and statistical data analysis of this study were conducted by MINITAB version 21.4.1. The optimization process with the RSM method consists of three primary phases: The statistical experimental design, the estimation of coefficients within a mathematical model, and the prediction of

responses along with an evaluation or validation of the model's adequacy. However, the Box-Behnken approach's experimental design is implemented to identify and evaluate the significant factors or parameters affecting the response [27]. Three factors (*A*, *B*, and *C*) were incorporated for selection, with each factor represented at 3 different levels. These levels must be designated as either "coded" or "uncoded" as shown in **Table 2**.

Table 2 Factors and levels as "coded" and "uncoded".

Factors	Level			Coded
	–1	0	1	
A, Pulp density (mg/L)	3	6	10	uncoded
B, Temperature (°C)	30	40	50	uncoded
C, Shaking rate (rpm)	120	150	180	uncoded

A second-order model can be represented through Eq. (2), which facilitates the estimation of its parameters. *Y* (metal) represents the anticipated value of the response variable, while A, B, and C denote the influencing factors. The coefficients of the model are represented as a_0, a_1, a_2, a_3, $a_{1.1}$, $a_{2.2}$, $a_{3.3}$, $a_{1.2}$, $a_{2.3}$, and $a_{1.3}$.

$$Y = a_0 + a_1A + a_2B + a_3C + a_{1.1}A^2 + a_{2.2}B^2 + a_{3.3}C^2 + a_{1.2}AB + a_{2.3}BC + a_{1.3}AC \quad (2)$$

In the current SHCC, it is understood that metals will exist in oxide form to cover the alumina matrix (Al_2O_3) of the catalyst support. As indicated, the metals will be extracted through the action of organic acids generated by *Aspergillus* fungi; however, the alumina matrix remains unreactive to these acids. The process of metal leaching from the SHCC is characterized as a heterogeneous phenomenon that occurs at the boundary between solid and liquid phases. A chemical reaction or a diffusion mechanism may influence the kinetics of this heterogeneous reaction. The concept of shrink core format was utilized to assess the kinetics of leaching under optimal conditions. This model provides a mathematical framework for understanding solid-state reactions, wherein a solid material (in this case, metals) is progressively consumed through a chemical reaction, while the diffusion of reactants (organic acids) occurs through a diminishing core that envelops the unreacted material (alumina matrix). The simultaneous occurrence of the mechanisms through chemical interaction and/or the process of diffusion can be represented by Eqs. (3) - (4), respectively [13]. Where x is the leaching efficiency (k_c) refers to the rate constant of the chemical reaction (min^{-1}); k_d represents the rate constant of the diffusion process (min^{-1}), and t is the leaching time (min).

$$1 - (1-x)^{1/3} = k_c t \quad (3)$$

$$1 - 3(1-x)^{2/3} + 2(1-x) = k_d t \quad (4)$$

Spike recovery test for the analysis method of metal elements in culture medium using ICP-AES

To validate the accuracy of the analytical approach, a spike recovery test was performed on a high-matrix medium.

Spiked samples were prepared by adding single-element standard solutions and diluting culture media 20 times with 1 v/v% nitric acid. Unspiked samples were generated by diluting culture media 20 times with 1 v/v% nitric acid [28]. The results are presented in **Table 3**. The spike recovery rates for all elements were within ± 5%.

Table 3 Spike recovery test for metal analysis in high-matrix culture medium using ICP-AES.

Elements	Detection limit (µg L^{-1})	Spiked concentration (µg L^{-1})	Unspiked sample (µg L^{-1})	Spiked sample (µg L^{-1})	Spike recovery rate (%)
Al	0.04	0.5	1.36	1.88	104
Ni	0.008	0.25	0.112	0.352	96
Mo	0.007	0.1	0.039	0.14	101
Fe	0.01	5	0.90	5.69	96
Zn	0.02	10	1.7	11.6	99

Note: Spike recovery values within 95% - 105% indicate negligible matrix interference and confirm the accuracy of the ICP-AES measurements.

Results and discussion

Composition of SHCC

Analysis of the metal composition of the raw SHCC was examined using a handheld XRF analyzer, as detailed in **Table 4**. It is essential to highlight that this analyzer did not evaluate aluminum because of the naturally high limits of detection (LODs) related to this particular element. The analysis of the elements of the pretreated SHCC performed through ICP-AES indicated that aluminum (39%), molybdenum (15%), iron (14.2%), and nickel (14.1%) are the predominant elements present. Additionally, zinc was detected as a minor component at a concentration of 640 ppm. The analysis revealed that the metal content determined by the XRF analyzer consistently exceeded that obtained through ICP-AES. This difference occurs because XRF evaluates the metal content directly from the solid catalyst, whereas ICP-AES necessitates the extraction of metal content via acid digestion. The total extraction of metal content from the catalyst through acid digestion could not be accomplished [15,29].

Table 4 Metal composition of SHCC.

Metals	Raw SHCC* (%)	Pretreated SHCC** (%)
Al	---	39.00 ± 0.55
Mo	19.6 ± 2.20	15.00 ± 0.75
Ni	19.88 ± 2.50	14.10 ± 0.30
Fe	18.78 ± 1.50	14.20 ± 0.62
Zn	0.07 ± 0.02	0.064 ± 0.04
	*XRF analyzer	**ICP-AES

Identification of fungi

From soil samples, five fungal species with different morphotaxa were isolated; however, only one strain was able to grow in PDA medium containing 0.5% (w/v) SHCC; hence, this strain was selected for morphological and molecular investigation. The morphological characteristics of the selected strain are that the fungus produces dark brown to black external conidiosphores with a subspheroidal shape. For the molecular confirmation of the selected strain, the nucleotide sequence of PCR products was determined by comparing the sequence data with the National Center for Biotechnology Information (NCBI) database. The nucleotide sequence of the selected strain exhibited 100% identity with *Aspergillus aculeatus* (GenBank accession number NR_111412.1). Filamentous fungi that are resistant to heavy metals are often found in soil samples taken from mine tailings because these organisms have adapted to live in contaminated environments. These fungi have enormous potential for biohydrometallurgy and bioremediation. Specifically, those belonging to the genus *Aspergillus* exhibited

varying levels of tolerance to different metals across a range of concentrations [28,29]. Because of this, fungi of this genus are commonly utilized in bioleaching to recover valuable metals from a variety of sources, including battery wastes, spent catalysts, and electronic waste, or e-waste [5,30,31].

Characterization of culture medium filtrate and leaching mechanism

The results indicate that *A. aculeatus* lowers the pH of its nutritive environment as it grows during the cultivation period, while the two main organic acids present in the medium at this time were citric acid and oxalic acid (**Figure 1**). Fundamental mechanisms are primarily involved in creation of these acids by *A. aculeatus* were (a) the emission of protons through the action of the ATPase which is responsible for proton translocation across the plasma membrane, which can serve as an indicator of growth; (b) the absorption of nutrients in return for protons; (c) the secretion of organic acids; and (d) the acidity condition from carbon dioxide generated during the fungal respiration. Citric acid is synthesized via the glycolytic pathway. The pathways of the pentose phosphate and glycolytic pathways enable *Aspergillus* species to utilize glucose and various carbohydrates for biosynthesis and cellular upkeep. It has been established that pyruvate kinase plays a crucial regulatory role in the synthesis of citric acid. In *Aspergillus* spp., oxalic acid biosynthesis primarily takes place through the transformation of oxaloacetate. This compound is generated by the enzyme pyruvate carboxylase acting on pyruvate, as a glycolysis product [34-39].

According to the findings of this study, oxalic acid and citric acid are fungal metabolites that are crucial for leaching. The mechanism of metal dissolution in this leaching occurs through two reactions. The first reaction entails substituting metal ions with hydrogen ions, commonly referred to as acidolysis, whereas the second reaction relates to the creation of complexes, known as complexolysis [12,13,40]. The hydrogen ions produced by these acids facilitate the movement of metal ions, whereas the chelation of metals ensures their stabilization within the solution. Organic acids significantly contribute to the enhanced detachment of metals from the surfaces of spent catalysts. The processes of hydrogen dissolution and complexolysis for these acids can be illustrated as follows, with Met^{n+} representing a metallic ion of a particular valence [41]. Eq. (5) through 10 depict the reactions related to the acidolysis and complexolysis processes of citric acid. The acid dissociation constants, represented as *pKa* values, for reactions 5 - 7 are 3.09, 4.75, and 6.40, respectively. The product entities present in Eqs. (8) - (10) are citric metallic complexes [41,42].

$$C_6H_8O_7 \longrightarrow (C_6H_7O_7)^- + H^+ \quad (5)$$

$$(C_6H_7O_7)^- \longrightarrow (C_6H_6O_7)^{2-} + H^+ \quad (6)$$

$$(C_6H_6O_7)^{2-} \longrightarrow (C_6H_5O_7)^{3-} + H^+ \quad (7)$$

$$n[(C_6H_7O_7)^-] + Met^{n+} \longrightarrow Met\,[(C_6H_7O_7)]_n \quad (8)$$

$$n[(C_6H_6O_7)^{2-}] + 2Met^{n+} \longrightarrow Met_2[(C_6H_6O_7)]_n \quad (9)$$

$$n[(C_6H_5O_7)^{3-}] + 3Met^{n+} \longrightarrow Met_3[(C_6H_5O_7)]_n \quad (10)$$

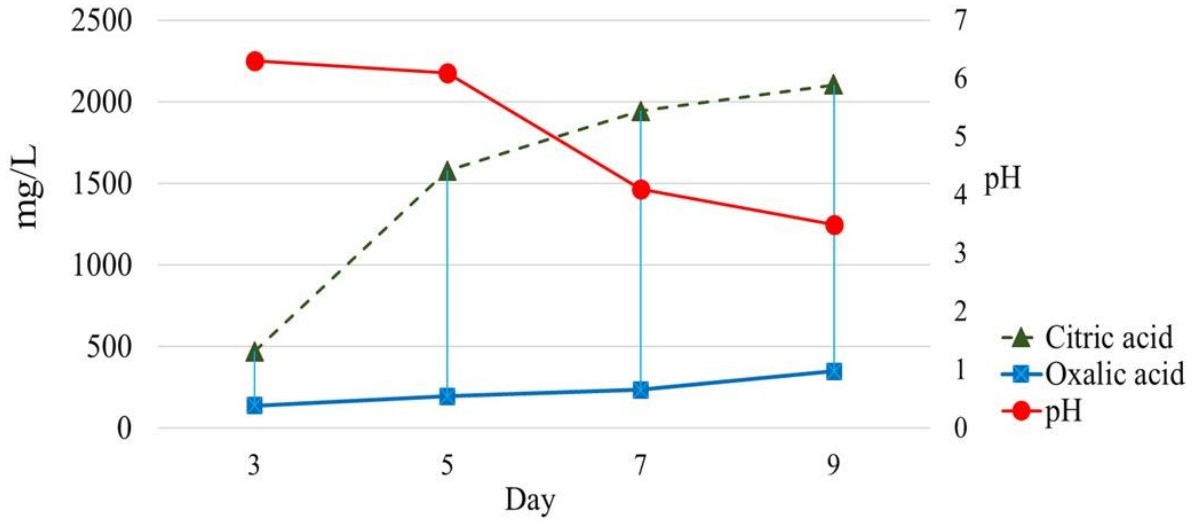

Figure 1 Alterations in organic acids concentrations and pH levels throughout the incubation period of *A. aculeatus*.

The reactions related to the acidolysis and complexolysis of oxalic acid are described in equations 11 through 14. The *pKa* values, which indicate the acid dissociation constants for reactions 11 and 12, are 1.25 and 4.14, respectively. $Met[(C_2HO_4)]_n$ and $Met_2[(C_2O_4)]_n$ took place in Eqs. (13) - (14), are oxalic metallic complexes [41].

$$C_2H_2O_4 \longrightarrow (C_2HO_4)^- + H^+ \quad (11)$$

$$(C_2HO_4)^- \longrightarrow (C_2O_4)^{2-} + H^+ \quad (12)$$

$$n[(C_2HO_4)^-] + Met^{n+} \longrightarrow Met[(C_2HO_4)]_n \quad (13)$$

$$n[(C_2O_4)^{2-}] + 2Met^{n+} \longrightarrow Met_2[(C_2O_4)]_n \quad (14)$$

Process optimization and kinetics study

The variables employed in this study included pulp density, temperature, and shaking rate, each evaluated at three coded levels/tiers (−1, 0, and +1). To identify the optimal tier of variables, RSM or response surface methodology was implemented, utilizing the BBD approach. The comprehensive experimental plan detailing the actual and coded values, along with the corresponding results from the BBD experiments, is presented in **Table 5**. The values of the response (*Y*) for all trials represent the mean value of the triplicate measurements. In this controlled experiment, the metal recoveries for Al, Ni, Mo, Fe, and Zn were 0.05%, 0.08%, 0.03%, 0.03%, and 0.02%, respectively. These values were considered insignificant, caused by the medium condition, which was controlled at pH 6.5. The statistical results provided by MINITAB indicate that the ANOVA for all response surface models is illustrated in **Table 6**. The value of prop > *F* for all models, which are below 0.05, confirms their statistical significance with a 95% confidence interval. The *F*-test values for the models of Y_{Al}, Y_{Ni}, Y_{Mo}, Y_{Fe}, and Y_{Zn} were determined to be 24.52, 16.87, 6.70, 4.95, and 8.72, respectively. To assess the effectiveness of a statistical model in predicting an outcome, the coefficient of determination, commonly referred to as R^2. According to **Table 6**, every R^2 value supports how well equations 15 through 19 represent the data, showing the model's adequacy in fitting the data. The coefficient of variation percentage (C.V.%) for all models ranges from 10% to 20%, indicating a satisfactory fit of the models [43,44]. The "Lack of fit" in equation *Y* shows the difference between the real measurements and the model's predicted values. "Lack of fit prop > *F*" for nearly all models is greater than 0.05, indicating that the models fit sufficiently, except for model Y_{Al}, which fits poorly at 0.018. The model form may not be appropriate for Al leaching, or the regression equation of Al might not accurately represent the underlying connection in the data. The detailed second-order polynomial equations related to metal leaching are represented by Eqs. (15) - (19).

$$Y_{Al} = 7.961 + 1.588A - 0.167B + 0.376C - 0.988A^2 - 0.374B^2 - 0.334C^2 - 0.029AB - 0.510BC + 0.251AC \quad (15)$$

$$Y_{Ni} = 4.728 + 0.811A + 0.065B + 0.200C - 0.558A^2 - 0.097B^2 - 0.352C^2 + 0.329AB + 0.020BC - 0.012AC \quad (16)$$

$$Y_{Mo} = 16.531 + 3.403A + 0.280B + 0.135C + 2.779A^2 - 0.114B^2 - 1.781C^2 + 1.452AB - 0.310BC + 0.285AC \quad (17)$$

$$Y_{Fe} = 10.829 + 1.414A + 0.179B - 0.021C - 1.011A^2 + 0.701B^2 - 0.050C^2 - 0.209AB - 0.380BC + 0.123AC \quad (18)$$

$$Y_{Zn} = 0.694 + 0.127A + 0.0585B + 0.003C + 0.061A^2 + 0.007B^2 - 0.021C^2 - 0.016AB - 0.004BC + 0.002AC \quad (19)$$

Table 5 Box-Behnken design and results of metal recovery yield.

Run	*A* Pulp density (mg/L)	*B* Temperature (°C)	*C* Shaking rate (rpm)	% Metal recovery				
				Al	Ni	Mo	Fe	Zn
1	–1 (3)	–1 (30)	0 (150)	5.07	3.64	16.09	8.43	0.57
2	1 (10)	–1 (30)	0 (150)	8.25	4.39	21.55	11.72	0.90
3	–1 (3)	1 (50)	0 (150)	5.01	3.09	14.40	9.74	0.66
4	1 (10)	1 (50)	0 (150)	8.07	5.17	25.66	12.19	0.93
5	–1 (3)	0 (40)	–1 (120)	5.15	2.60	15.17	8.58	0.64
6	1 (10)	0 (40)	–1 (120)	7.88	4.40	19.86	11.11	0.85
7	–1 (3)	0 (40)	1 (180)	4.90	3.21	14.63	8.18	0.61
8	1 (10)	0 (40)	1 (180)	8.63	5.06	20.46	11.20	0.83
9	0 (6)	–1 (30)	–1 (120)	6.39	4.14	14.34	11.15	0.57
10	0 (6)	1 (50)	–1 (120)	6.86	4.25	14.87	11.74	0.75
11	0 (6)	–1 (30)	1 (180)	8.66	4.27	15.47	11.98	0.62
12	0 (6)	1 (50)	1 (180)	7.09	4.46	14.77	11.05	0.78
13	0 (6)	0 (40)	0 (150)	7.96	4.84	15.03	10.18	0.69
14	0 (6)	0 (40)	0 (150)	7.90	4.80	16.06	11.98	0.71
15	0 (6)	0 (40)	0 (150)	8.02	4.54	18.50	10.33	0.68

Table 6 ANOVA for RSM.

	Y_{Al}	Y_{Ni}	Y_{Mo}	Y_{Fe}	Y_{Zn}
Model *F*-value	24.52	16.87	6.70	4.95	8.72
Model prob > *F*	0.001	0.003	0.025	0.047	0.014
R^2	0.98	0.97	0.92	0.90	0.94
C.V. %	19.90	17.83	19.62	12.73	16.04
Lack of fit prob > *F*	0.018	0.306	0.672	0.891	0.060

The leaching levels of metals are represented in the surface plots shown in **Figure 2**. The gradient of the surface reflects how much the experimental factors affect the response value. A high gradient value signifies a substantial impact of the experimental factor on the response [45]. A spent catalyst density (a density of pulp) is important for affecting the leaching of Mo, Fe, Al, Ni, and Zn, arranged in descending order of their leaching rate. Temperature and shaking rate exhibit a limited interaction with pulp density in improving the Al leaching rate; the relationship between temperature and shaking rate greatly affects the leaching of Al. The

impact of temperature and shaking rate on the interaction with the density of pulp is relatively limited, akin to the leaching of Ni. Additionally, there is no interaction between temperature and shaking rate throughout the recovery process. The recovery rate of Mo, Fe, and Zn is primarily influenced by pulp density. In Mo leaching, the temperature remains unaffected by the shaking rate, and conversely, the shaking rate does not impact the temperature during the Fe leaching process. The temperature has a combined effect on pulp density in the leaching of Zn, whereas the shaking rate exhibits minimal interaction with both pulp density and temperature. According to the response optimization, which was analyzed using MINITAB, the projected maximum recoveries for Al, Ni, Mo, Fe, and Zn were determined to be 7.98%, 5.27%, 24.55%, 11.92%, and 0.93%, as detailed in **Table 7**.

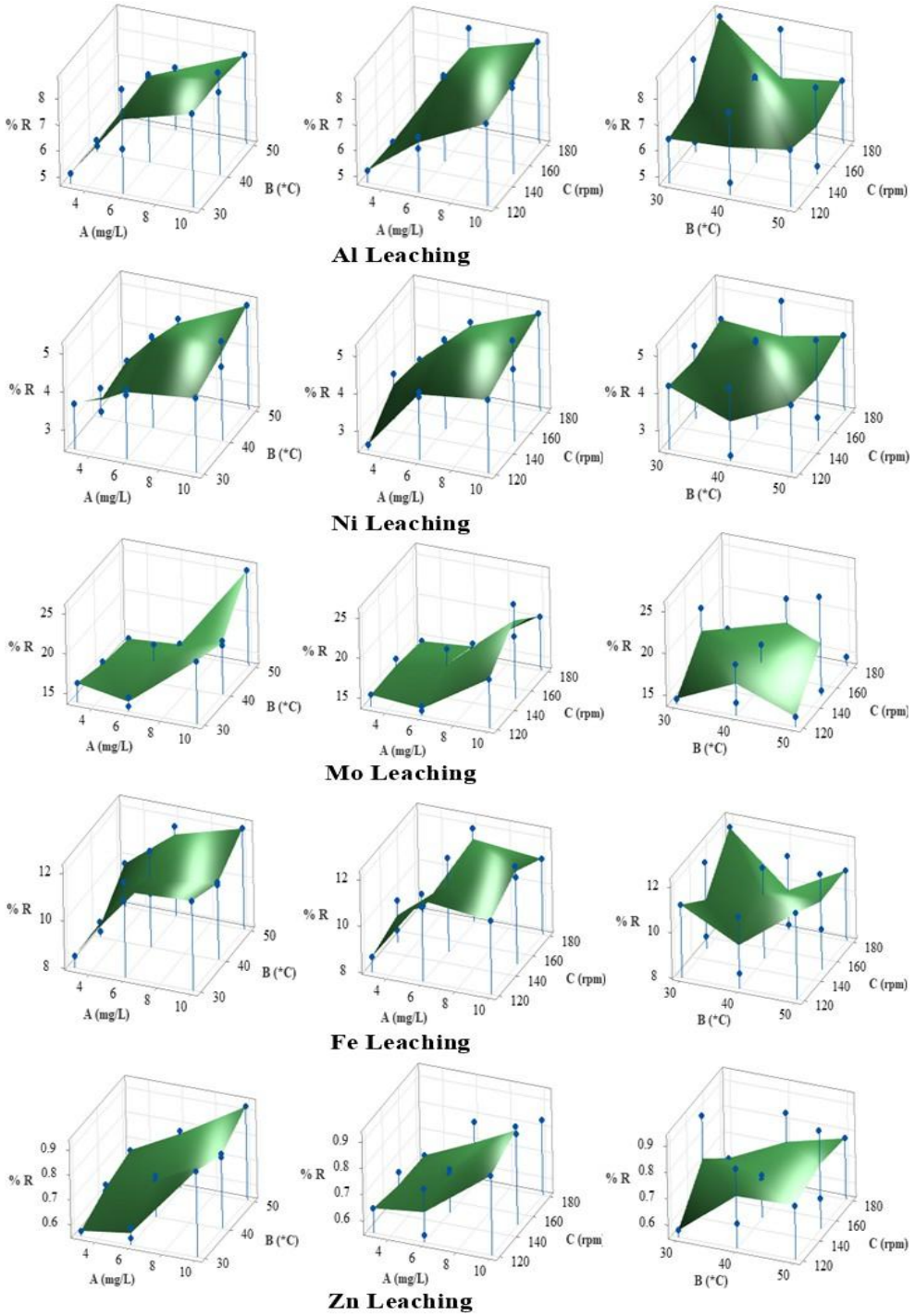

Figure 2 Surface plots: Impact of the density of pulp (A), temperature (B), and shaking rate (C) on metal leaching (% R).

Table 7 Predicted values and experimental values.

Metal recovery	Goal	Predicted value (%)	Experimental value (%)	Controlled value (%)	Confidence Interval (95%)	
					Low	High
Al	Maximum	7.98	8.10 ± 0.20	0.30+0.03	7.205	8.763
Ni	Maximum	5.27	4.98 ± 0.20	0.35 + 0.03	4.769	5.763
Mo	Maximum	24.55	22.95 ± 0.80	0.35 + 0.07	21.08	28.02
Fe	Maximum	11.92	12.02 ± 0.35	0.32 + 0.15	10.311	13.519
Zn	Maximum	0.93	0.92 ± 0.05	0.03 + 0.01	0.8268	1.0374

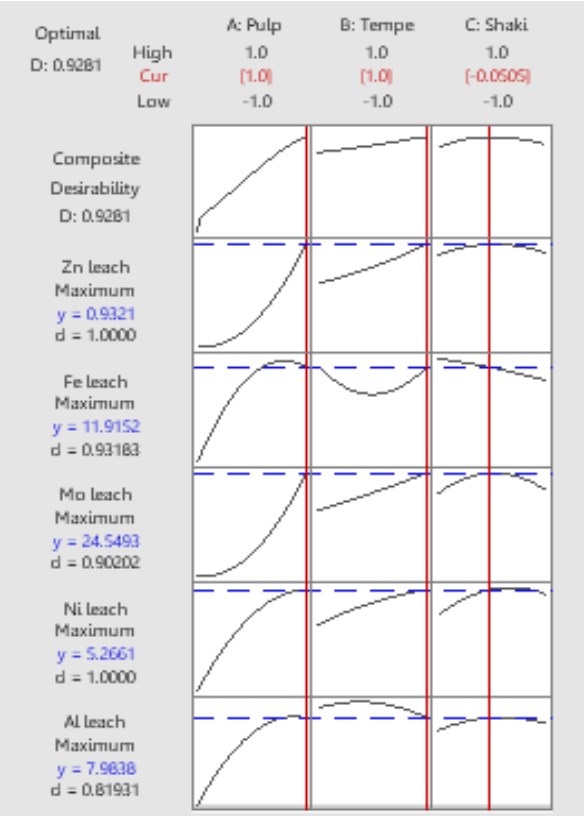

Figure 3 Response optimization for maximum recoveries of Al, Ni, Mo, Fe, and Zn.

According to the response optimization chart presented in **Figure 3**, at a composite desirability (D) of 0.9281, the recognized optimal conditions for these recoveries, expressed in coded form, were (1), (1), and (–0.0505) corresponding to pulp density, temperature, and shaking rate, respectively. The optimal parameters determined were a spent catalyst density of 10% (weight per volume), a temperature of 50 °C, and a shaking rate of 148 revolutions per min. Independent leaching experiments were conducted under optimal conditions to validate this prediction. The experiment results indicate that the validation experiments are closely aligned with the predicted values derived from the fitted correlations, maintaining a 95% confidence interval. The amount of metal recovery from the control experiment could be attributed to the pH level of the culture broth, which was refined to 6.5 using hydrochloric acid (2 N) during the preparation process of the culture medium filtrate. This research is consistent with previous findings on the extraction of platinum from spent refinery catalysts through a hybrid method involving oxalic acid produced by *A. niger* [9].

Additionally, it supports the recovery of nickel, molybdenum, and iron from used hydrocracking catalysts with the aid of modified *A. niger* [14,15]. Furthermore, this study is in agreement with the bioleaching of aluminum from spent fluid catalytic cracking catalysts using various *Aspergillus* species. The findings from the experiments conducted in this study align with previous research that utilized *A. niger* for optimizing processes and modeling the extraction of heavy metals from a molybdenum-rich spent catalyst through response surface methodology [46]. The prediction of the leaching mechanism will be made using the intended model based on experimental data. The decision-making process can be streamlined by using these models to supply trustworthy data for initial feasibility studies.

The study of reaction control on the surface of catalysts is important because the chemical reactions, or dissolving metals with organic acids, and the diffusion or movement through pores/catalyst layers, are key processes in metal leaching, with one often being the rate-limiting step or a combination of both dictating efficiency by controlling how quickly valuable metals separate from catalyst waste. Reactions break down the solid matrix, while diffusion transports dissolved ions away, forming a dynamic interplay for metal recovery. In this study, kinetic analysis was conducted by fitting experimental data to the shrinking core model. The surface chemical reaction control model provided higher coefficients of determination compared with the diffusion-controlled model, indicating that surface reactions were the dominant rate-limiting step under the studied conditions. Kinetic rate constants were obtained from the slopes of the fitted linear plots. Although uncertainty estimates were not explicitly reported, the consistency of model fitting supports the reliability of the kinetic interpretation. This kinetic study is based on the principles of the shrinking core model [47,48]. According to the data in **Table 8** and the graph in **Figure 4**, a comparative analysis of the correlation coefficients (R^2) reveals that the chemical control reaction, represented by the graphs in group A, exhibits a closer approximation to linearity than the diffusion process depicted in group B. The equations representing the lines of best fit are arranged in a descending sequence according to the elements Ni, Zn, Al, Fe, and Mo, such that the arrangement in group A aligns with that in group B. The k_c (surface chemical reaction rate constant) and the k_d (the rate constant of the diffusion process) can be ascertained through the gradient or slope of the line. The metals molybdenum, iron, aluminum, nickel, and zinc demonstrate varying rates of leaching that can be organized in descending order, starting with the highest and progressing to the lowest.

Although *A. niger* has been widely investigated in fungal bioleaching systems, the present study emphasizes the use of a cell-free culture filtrate of *A. aculeatus*, which enables clearer mechanistic interpretation without interference from fungal biomass adsorption or surface binding effects. This simplified chemical environment allows more direct evaluation of acidolysis and complexolysis driven dissolution mechanisms compared to whole-cell systems.

The metal recovery efficiencies obtained in this study were moderate relative to previous whole-cell bioleaching reports. However, the present work was designed to evaluate the feasibility and kinetic behavior of metal dissolution using a cell-free culture filtrate under controlled and mild conditions. The comparatively lower recoveries likely reflect the absence of direct fungal solid interactions and biomass associated mechanisms. Therefore, the proposed approach should be regarded as a complementary or pre-treatment strategy rather than a standalone high-efficiency recovery process. From a practical perspective, although detailed techno-economic analysis was beyond the scope of this study, the use of a cell-free culture filtrate under mild operating conditions may offer potential advantages in terms of lower energy demand and simplified downstream processing compared to conventional high-temperature hydrometallurgical treatments.

In terms of mechanistic interpretation, the proposed dissolution mechanism is supported by consistent evidence from organic acid identification, pH evolution, and kinetic modeling using the shrinking core model. These complementary findings indicate that metal leaching is predominantly governed by surface chemical reactions. Nevertheless, direct surface characterization techniques such as SEM/EDS analysis before and after leaching would further strengthen experimental validation of the proposed mechanism. This aspect is recognized as a limitation of the present study. Moreover, a comprehensive thermodynamic

evaluation of metal organic acid interactions, such as Eh–pH diagram analysis or Gibbs free energy assessment, was beyond the scope of the present study. The current work primarily focused on experimentally observed leaching behavior and kinetic interpretation under controlled conditions. Incorporation of thermodynamic modeling would further improve understanding of metal speciation and stability and is therefore recommended for future investigations.

Table 8 Best-fit equations and correlation coefficients by shrink core model.

Metal leaching	Surface chemical reaction – Graph A Best-fit equation	Diffusion – Graph B Best-fit equation
Mo	y = 0.0827x - 2.1449 (R^2 = 0.9119)	y = 0.0184x - 0.648 (R^2 = 0.8018)
Fe	y = 0.0418x - 1.0122 (R^2 = 0.9273)	y = 0.0048x - 0.1627 (R^2 = 0.8317)
Al	y = 0.0297x - 0.6991 (R^2 = 0.9367)	y = 0.0025x - 0.0801 (R^2 = 0.8535)
Ni	y = 0.0173x - 0.4216 (R^2 = 0.9440)	y = 0.0008x - 0.0262 (R^2 = 0.8704)
Zn	y = 0.0038x - 0.0876 (R^2 = 0.9412)	y = 0.00004x - 0.0013 (R^2 = 0.8676)

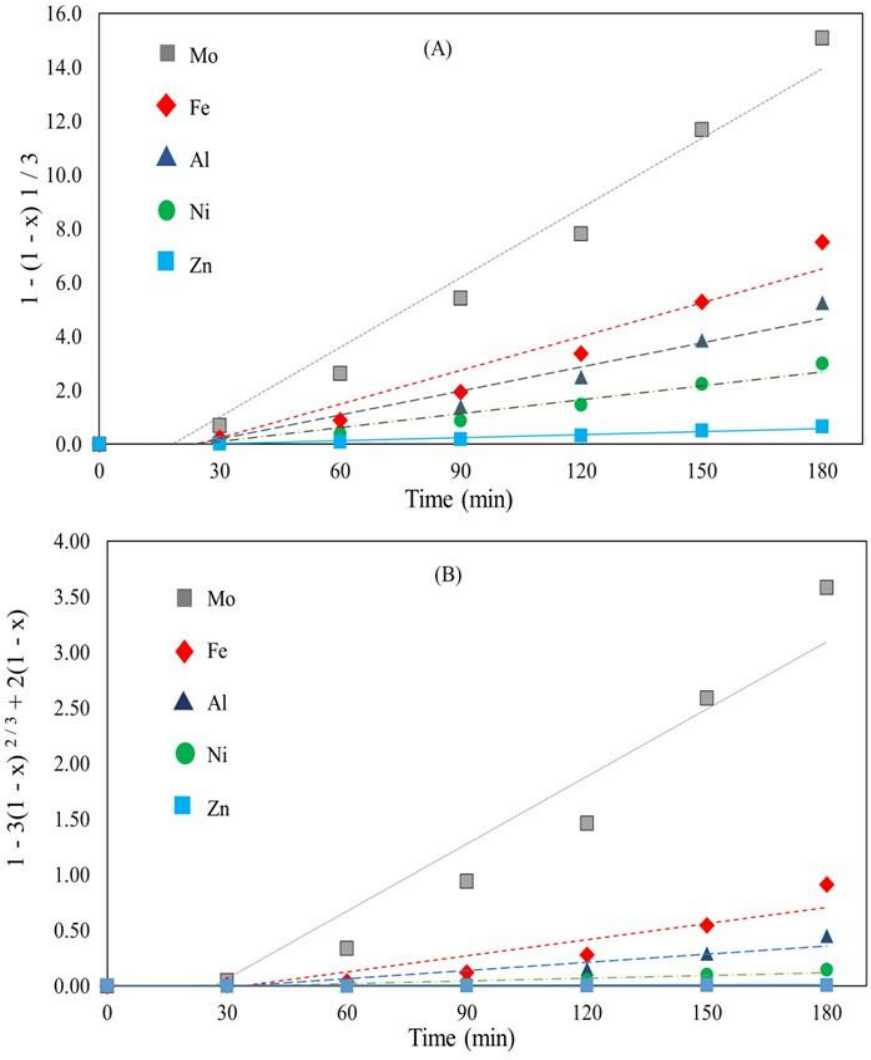

Figure 4 (A) Surface chemical reaction equation [1-(1-x)$^{1/3}$] versus time, and (B) diffusion equation [1-3(1-x)$^{2/3}$ + 2(1-x)] versus time for bioleaching of Al, Ni, Mo, Fe, and Zn from SHCC by culture medium filtrate of *Aspergillus aculeatus*.

Conclusions

In this research, *A. aculeatus* is a fungus that was isolated from soil contaminated with heavy metals in gold mine tailings in Thailand. The filtrate derived from the culture medium of these isolated fungi was utilized to extract heavy metals from SHCC. Fungus produces citric acid and oxalic acid throughout the incubation phase. Organic acids are essential in the processes of acidolysis and complexolysis, which are fundamental reactions in the metal leaching process. The optimization of the leaching process with the Box–Behnken design led to enhanced extraction effectiveness of Al, Ni, Mo, Fe, and Zn from the SHCC. Notably, the impact of parameters pulp density, temperature, and shaking rate during the leaching process exhibited significant variability, as evidenced by the differing response values obtained. The response values indicated in each metal trial's polynomial equations (Y) were verified using an ANOVA approach. Except for the model of Al leaching, which fits poorly, the models of Fe, Mo, Ni, and Zn fit well. Future research should consider different model structures, such as non-linear ones, to better fit the data. In the optimal conditions established for the process, a culture filtrate ratio of 10% (w/v) of SHCC, a temperature of 50 °C, and a rotation rate of 148 rpm yielded the following order of metal leaching recoveries from highest to lowest: Mo, Fe, Al, Ni, and Zn. The investigation of kinetics through the shrinking core model revealed that the mechanism of metal leaching is mainly governed by surface chemical reactions rather than diffusion processes.

Although the metal recovery yields obtained in this study were moderate and lower than those reported in studies employing whole fungal cells, the use of cell-free fungal culture filtrate enabled substantially shorter leaching times and simplified operational control. These results suggest that the proposed approach is more suitable as a complementary or pre-treatment step rather than a standalone large-scale metal recovery process. Future studies should explicitly address scale-up challenges by investigating strategies such as increasing organic acid concentrations, repeated or continuous use of culture filtrate, integration with mild pretreatment methods, and evaluation under continuous or semi-continuous reactor systems. Such investigations are necessary to better assess the industrial applicability of fungal culture filtrate-based leaching as an alternative to conventional pyro-hydro-metallurgical processes.

Acknowledgements

The authors would like to thank the Department of Chemical Engineering, Faculty of Engineering, and the Faculty of Science and Technology, Pathumwan Institute of Technology, for their academic and research support. The authors also sincerely thank NICS Company, Rayong Province, Thailand, for providing the spent hydrocracking catalyst used in this study.

Declaration of Generative AI in Scientific Writing

The author certifies that no content was generated or data interpreted by AI, except for the use of creative AI to help correct grammar.

CRediT Author Statement

Thanakorn Sawangchart: Methodology, Formal analysis, Investigation, Data curation, and Writing – original draft. **Bunyarit Meksiriporn**: Data curation and Supervision. **Thanawat Sutjaritvorakul**: Conceptualization, Project administration, Resources, Funding acquisition, Supervision, Validation, and Writing – original draft.

References

[1] International Energy Agency, Available at: https://iea.blob.core.windows.net/assets/c00d5f19-f52f-47c1-82aa-6a464a688593/-16MAY2023_OilMarketReport.pdf, accessed March 2023.

[2] P Miao, X Zhu, Y Guo, J Miao, M Yu and C Li. Combined mild hydrocracking and fluid catalytic cracking process for efficient conversion of light cycle oil into high-quality gasoline. *Fuel* 2021; **292**, 120364.

[3] A Pathak, M Vinoba and R Kothari. Emerging role of organic acids in leaching of valuable metals from refinery-spent hydroprocessing catalysts, and potential techno-economic challenges: A review. *Critical Reviews in Environmental Science and Technology* 2020; **51(1)**, 1-43.

[4] M Marafi and A Stanislaus. Spent catalyst waste management: A review Part I-Developments in hydroprocessing catalyst waste reduction and use.

Resources, Conservation and Recycling 2008; **52(6)**, 859-873.

[5] S Das, NN Deshavath, VV Goud and VV Dasu. Bioleaching of Al from spent fluid catalytic cracking catalyst using *Aspergillus* species. *Biotechnology Reports* 2019; **23**, e00349.

[6] N Nagar, H Garg and CS Gahan. Integrated bio-pyro-hydro-metallurgical approach to recover metal values from petroleum refinery spent catalyst. *Biocatalysis and Agricultural Biotechnology* 2019; **20**, 101252.

[7] T Sutjaritvorakul, GM Gadd, K Suntornvongsagul, AJS Whalley, S Roengsumran and P Sihanonth. Solubilization and transformation of insoluble zinc compounds by fungi isolated from a zinc mine. *EnvironmentAsia* 2013; **6(2)**, 42-46.

[8] T Sutjaritvorakul, GM Gadd, AJS Whalley, K Suntornvongsagul and P Sihanonth. Zinc oxalate crystal formation by *Aspergillus nomius*. *Geomicrobiology Journal* 2016; **33**, 289-293.

[9] P Phogat, S Kumar and M Wan. A scientometrics study of advancing sustainable metal recovery from e-waste: Processes, challenges, and future directions. *RSC Sustainability* 2025; **3**, 2434-2454.

[10] H Malekian, M Salehi and D Biria. Investigation of platinum recovery from a spent refinery catalyst with a hybrid of oxalic acid produced by *Aspergillus niger* and mineral acids. *Waste Management* 2019; **85**, 264-271.

[11] MH Muddanna and SS Baral. A comparative study of the extraction of metals from the spent fluid catalytic cracking catalyst using chemical leaching and bioleaching by *Aspergillus niger*. *Journal of Environmental Chemical Engineering* 2019; **7(5)**, 103335.

[12] MH Muddanna and SS Baral. Leaching of nickel and vanadium from the spent fluid catalytic cracking catalyst by reconnoitering the potential of *Aspergillus niger* associating with chemical leaching. *Journal of Environmental Chemical Engineering* 2019; **7(2)**, 103025.

[13] F Amiri, SM Mousavi, S Yaghmaei and M Barati. Bioleaching kinetics of a spent refinery catalyst using *Aspergillus niger* at optimal conditions. *Biochemical Engineering Journal* 2012; **67**, 208-217.

[14] F Amiri, SM Mousavi and S Yaghmaei. Enhancement of bioleaching of a spent Ni/Mo hydroprocessing catalyst by *Penicillium simplicissimum*. *Separation Purification Technology* 2011; **80(3)**, 566-576.

[15] F Amiri, S Yaghmaei, SM Mousavi and S Sheibani. Recovery of metals from spent refinery hydrocracking catalyst using adapted *Aspergillus niger*. *Hydrometallurgy* 2011; **109(1-2)**, 65-71.

[16] D Santhiya and YP Ting. Use of adapted *Aspergillus niger* in the bioleaching of spent refinery processing catalyst. *Journal of Biotechnology* 2006; **121(1)**, 62-74.

[17] D Santhiya and YP Ting. Bioleaching of spent refinery processing catalyst using *Aspergillus niger* with high-yield oxalic acid. *Journal of Biotechnology* 2005; **116(2)**, 171-184.

[18] KHM Aung and YP Ting. Bioleaching of spent fluid catalytic cracking catalyst using *Aspergillus niger*. *Journal of Biotechnology* 2005; **116(2)**, 159-170.

[19] M Islam and YP Ting. Fungal bioleaching of spent hydroprocessing catalyst: Effect of decoking and particle size. *Advanced Material Research* 2009; **71-73**, 665-668.

[20] NH Aziz and N Zainol. Isolation and identification of soil fungi isolates from forest soil for flooded soil recovery. *IOP Conference Series: Materials Science and Engineering* 2018; **342**, 012028.

[21] JA Sayer, SL Raggett and GM Gadd. Solubilization of insoluble metal compounds by soil fungi: Development of a screening method for solubilizing ability and metal tolerance. *Mycological Research* 1995; **99(8)**, 987-993.

[22] MA Formina, IJ M., Alexander, JV Colpaert and GM Gadd. Solubilization of toxic metal minerals and metal tolerance of mycorrhizal fungi. *Soil Biology Biochemistry* 2005; **37(5)**, 851-866.

[23] HL Barnett and BB Hunter. *Illustrated genera of imperfect fungi*. 4th ed. APS Press, Minnesota, 1998.

[24] CR Lefevre, MN Diouf, A Brauman and M Neyra. Phylogenetic relationships in *Termitomyces* (Family agaricaceae) based on the nucleotide sequence of ITS: A first approach to elucidate the evolutionary history of the symbiosis between fungus-growing termites and their fungi.

Molecular Phylogenetics and Evolution 2002; **22(3)**, 423-429.

[25] LT Vargas, MER Carmona and YV Salazar. Determination of citric and oxalic acid in fungi fermentation broth through HPLC-DAD and solid-phase extraction. *DYNA* 2020; **87**, 26-30.

[26] T Junhuathoen, T Somdee and C Aiyathiti. Isolation and selection of copper bioleaching bacteria and optimization using response surface methodology on copper recovery from discarded printed circuit boards. *KKU Science Journal* 2021; **49(1)**, 7-18.

[27] L Ren, B Liu, S Bao, W Ding, Y Zhang, X Hou, C Lin and B Chen. Recovery of Li, Ni, Co and Mn from spent lithium-ion batteries assisted by organic acids: Process optimization and leaching mechanism. *International Journal of Minerals, Metallurgy and Materials* 2024; **31**, 518-530.

[28] RJ Graham, H Bhatia and S Yoon. Consequences of trace metal variability and supplementation on Chinese hamster ovary (CHO) cell culture performance: A review of key mechanism and considerations. *Biotechnology and Bioengineering* 2019; **116(12)**, 3446-3456.

[29] P Hannaker, M Uaunu and SK Sen. Comparative study of ICP-AES and XRF analysis of major and minor constituents on geological materials. *Chemical Geology* 1984; **42(1-4)**, 319-324.

[30] CLVăcar, E Covaci, S Chakraborty, B Li, DC Weindorf, T Frențiu, M Pârvu and D Podar. Heavy metal-resistant filamentous fungi as potential mercury bioremediators. *Journal of Fungi* 2021; **7(5)**, 386.

[31] R Nofiani, R Mu'in, Hafizah and P Ardiningsih. Bioremoval of Pb^{2+} by *Aspergillus niger* D1RA, A heavy metal-resistant fungus isolated from an illegal gold mining site. *Biodiversitas Journal of Biological Diversity* 2024; **25(8)**, 2504-2511.

[32] T Chandakhiaw, N Teaumroong, P Piromyou, P Songwattana, W Tanthanuch, S Tancharakorn and S Khumkoa. Efficiency of *Penicillium* sp. and *Aspergillus* sp. for bioleaching lithium cobalt oxide from battery wastes in potato dextrose broth and sucrose medium. *Results Engineering* 2024; **24**, 103170.

[33] A Trivedi and S Hait. Fungal bioleaching of metals from WPCBs of mobile phones employing mixed *Aspergillus* spp.: Optimization and predictive modelling by RSM and AI models. *Journal of Environmental Management* 2024; **394**, 119565.

[34] GM Gadd. Fungal production of citric and oxalic acid: Importance in metal speciation, physiology and biogeochemical processes. *Advances Microbial Physiology* 1999; **41**, 47-92.

[35] W Burgstaller and F Schinner. Leaching of metals with fungi. *Journal of Biotechnology* 1993; **27(2)**, 91-116.

[36] E Książek. Citric acid: Properties, microbial production, and applications in industries. *Molecules* 2024; **29(1)**, 22.

[37] CP Kubicek, G Schreferl-Kunar, W Wöhrer and M Röhr. Evidence for a cytoplasmic pathway of oxalate biosynthesis in *Aspergillus niger*. *Applied and Environmental Microbiology* 1988; **54(3)**, 633-637.

[38] GM Gadd, J Bahri-Esfahani, Q Li, YJ Rhee, Z Wei, M Fomina and X Liang. Oxalate production by fungi: Significance in geomycology, biodeterioration and bioremediation. *Fungal Biology Reviews* 2014; **28(2-3)**, 36-55.

[39] T Watanabe, N Shitan, S Suzuki, T Umezawa, M Shimada, K Yazaki and T Hattori. Oxalate efflux transporter from the brown rot fungus *Fomitopsis palustris*. *Applied and Environmental Microbiology* 2010; **76**, 23.

[40] L Dusengemungu, G Kasali, C Gwanama and B Mubemba. Overview of fungal bioleaching of metals. *Environmental Advances* 2021; **5**, 100083.

[41] F Faraji, R Golmohammadzadeh, F Rashchi and N Alimardani. Fungal bioleaching of WPCBs using *Aspergillus niger*: Observation, optimization and kinetics. *Journal of Environmental Management* 2018; **217**, 775-787.

[42] BJ Seh-Bardan, R Othman, SA Wahid, A Husin and F Sadegh-Zadeh. Bioleaching of heavy metals from mine tailings by *Aspergillus fumigatus*. *Bioremediation Journal* 2012; **16(2)**, 57-65.

[43] NR Draper and H Smith. *Applied regression analysis*. John Wiley & Sons, New York, 1998.

[44] AH Al-Marshadi, M Aslam and A Abdullah. Uncertainty-based trimmed coefficient of variation with application. *Journal of Mathematics* 2021; **2021**, 6.

[45] KP Bowman. *An introduction to programming with IDL interactive data language*. Elsevier Academic Press, Amsterdam, 2005.

[46] RM Gholami, SM Mousavi and SM Borghei. Process optimization and modeling of heavy metals extraction from a molybdenum-rich spent catalyst by *Aspergillus niger* using response surface methodology. *Journal of Industrial and Engineering Chemistry* 2012; **18(1)**, 218-224.

[47] S Keshavarz, F Faraji, F Rashchi and M Mokmeli. Bioleaching of manganese from a low-grade pyrolusite ore using *Aspergillus niger*: Process optimization and kinetic studies. *Journal of Environmental Management* 2021; **285**, 112153.

[48] M Saldaña, M Jeldres, FMG Madrid, S Gallegos, I Salazar, P Robles and N Toro. Bioleaching Modeling: A review. *Materials* 2023; **16**, 3812.